

Polystyrene Latex Nanoparticles Shrink When Polyelectrolyte of the Same Charge Is Added

Sangmin Jeon

Life Sciences Division, Oak Ridge National Laboratory, Oak Ridge, Tennessee 37831

Steve Granick*

Department of Materials Science, Chemistry, and Physics, University of Illinois, Urbana, Illinois 61801

Received December 20, 2003; Revised Manuscript Received February 12, 2004

ABSTRACT: Reversible deswelling of latex nanoparticles, induced by electrostatic repulsion after adding polyelectrolyte (polystyrenesulfonate, PSS) chains of the same charge to suspensions of the particles in deionized water, is shown using time-resolved fluorescence depolarization of fluorescent dyes (Lumogen 5 Yellow 083) impregnated within the nanoparticles, using methods of two-photon excitation. Shrinkage of the particles produced closer spacing between dyes, thus enhancing fluorescence quenching and homo energy transfer, which depolarizes fluorescence emission. Thus, it was observed that the higher the PSS concentration, the more rapid decay of fluorescence depolarization on the subnanosecond time scale. When NaCl was subsequently added, screening caused the original particle size to be recovered. Tentatively, the diameter increase was roughly 7%. The spatial resolution provided by two-photon excitation implies that this method can be used to estimate the size changes of particles in situ in concentrated semiturbid solutions.

Introduction

The interaction between suspended colloidal particles and polymers in solution to which they fail to adsorb is an important niche topic in colloid science. For example, the presence of polymers near cross-linked polystyrene latex in good solvent is known to cause osmotic shrinkage of the latex particle.¹ However, the effect of electrostatic interaction between charged particles and polyelectrolytes on their conformation has not been studied to our best knowledge. As an example of relevance, this situation is common in biomaterials applications in cases where the adsorption of proteins should be avoided.

If the latex particles and the polyelectrolytes possess electrical charge of the same sign, electrostatic repulsion forces should influence their size and conformation. However, it is not so easy to detect such changes. Typically, particle size can be determined by electron microscopy, fluorescence depolarization, photon correlation spectroscopy, or scattering measurement.^{2–9} Otake and co-workers used dynamic light scattering to measure the swelling of the un-cross-linked polystyrene latex nanoparticles in water¹⁰ and observed that the latex particles swelled by 20% as CO₂ pressure was increased to 35 MPa. The increase in water was 1.6 times larger than that in air. On the basis of thermodynamic models, the enhanced swelling in water was attributed to the adsorption of CO₂ into the interfacial region, which lowers the overall interfacial tension between the latex and water phases.

Our experiments began with the hypothesis that electrostatic interactions might play a similar role. Reversible deswelling of latex nanoparticles impregnating fluorescent dyes was induced by electrostatic repulsion after adding polyelectrolyte chains of the same

charge to suspensions of the particles in water. Since light scattering is hard to apply for these turbid solutions, fluorescence spectroscopy was adopted here. Non-radiative fluorescence energy transfer was originally developed in the field of biology to measure the distance between donor and acceptor.^{11–13} The rate of fluorescence energy transfer from donor to acceptor is¹¹

$$k_T = \frac{1}{\tau_D} \left(\frac{R_0}{r} \right)^6 \quad (1)$$

where τ_D is the decay time of the donor in the absence of the acceptor, R_0 is the Förster distance, and r is the donor-to-acceptor distance. Therefore, energy transfer will be efficient when the transfer rate is faster than the lifetime of the donor.

Since the energy transfer rate is inversely proportional to the sixth power of the distance between donor and acceptor, it is very sensitive to small distance changes. On the basis of the fact that energy transfer depolarizes the fluorescence emission, two-photon excitation time-resolved fluorescence anisotropy (TRFA) was adopted here to detect size changes. Although the scattering medium can depolarize the fluorescence,^{14–16} it is overcome by adopting two-photon excitation confocal geometry that can control the focal point tightly near the wall of the sample cell to minimize scattering.

Experimental Section

Instruments. Time-resolved fluorescence depolarization is a method by which to quantify rotational relaxation times on the nanosecond time scale. In this way, rotational motions of a fluorescent molecule are used to probe the local microenvironment within which it resides.

Two-photon excitation of the fluorescent probe molecules was induced using a femtosecond Ti:sapphire laser (Mai Tai, Spectra-Physics) whose fwhm (full width at half-maximum) pulse was measured to be 100 fs. The repetition rate was 80

* Corresponding author. E-mail: sgranick@uiuc.edu.

MHz, and the wavelength was 800 nm. The experiments were performed within a homemade microscope and a perfusion chamber (Sigma) with 1.3 mm total thickness.

In the design that we employed, the vertically polarized laser beam was first split into two beams, and one of them was introduced into an objective lens (Mitutoyo, numerical aperture N.A. = 0.55) and focused onto the sample. The other beam was used as a trigger signal for the single photon counting system (Becker & Hickl GmbH, Berlin, Germany). The emitted fluorescence was collected by the same objective lens and focused again by a tube lens in order to increase the response of the photomultiplier tube (PMT) detectors. A fast PMT (Hamamatsu, R5600) and a photodiode were used to detect the fluorescence and the trigger signal, respectively. The PMT signal was input to the time-to-amplitude converter as a start signal followed by a constant fractional discriminator (Becker & Hickl GmbH, TCSPC730). In this setup the total instrument response function was around 150 ps.

To measure fluorescence emission spectra, a commercial instrument (QuantaMaster, Photon Technology International) was employed without modification.

Materials. The poly(styrenesulfonate) and the polystyrene latex particles were purchased from Polymer Laboratories (U.K.) and Interfacial Dynamics Corp., respectively, and used as received without any further purification. As given by the manufacturers, the weight-average molecular weights of the poly(styrenesulfonate) (PSS) samples were $M_w = 400\,000$ (PSS 400K) and $35\,000\text{ g mol}^{-1}$ (PSS 35K), and their polydispersity, weight-average relative to number-average molecular weight, was 1.1 in both cases. Poly(styrenesulfonate) was selected as the matrix molecule because of its large density of negative charge in deionized water and its similar molecular structure relative to polystyrene latex. The dry diameter of the latex particles was stated by the manufacturer to be 110 nm, and its final concentration in the colloid suspension was fixed at 45 nM. The molar mass of one polystyrene chain in latex particle is about 300 000, and one particle consists of approximately 1500 polystyrene chains. Both end groups of every chain are charged with sulfate groups.

As received, Lumogen F Yellow 083 (BASF) had been impregnated inside the particles under organic solvent. Although the detailed chemical composition of this proprietary dye is not known, it is known that it belongs to the family of perylene dyes, which are very hydrophobic. Indeed, a prior study from this laboratory using particles impregnated with the same dye showed no complications that would suggest solubility of this dye in the aqueous solution.⁶ Since 6 mg of dye was impregnated inside 1 g of latex particle (datum provided by Interfacial Dynamics Corp.), the average number of dyes in a particle and the distance between dyes corresponded to 4300 dyes/particle and 25 nm, respectively. However, this estimate of mean distance between dyes is rough because the molecular weight and dispersion of the dye inside the particles are not known precisely.

Results and Discussion

Figure 1 shows the fluorescence emission and excitation spectra of the labeled polystyrene latex. A member of the perylene family, it characteristically shows two peaks in its excitation and emission spectra. PSS 400K and PSS 35K were added to the colloidal solution and compared with each other. Although the emission peak at 522 nm shifts slightly to longer wavelength, the overall excitation and emission spectra are independent of the concentration and size of the polyelectrolytes. The inset of Figure 1 shows the wavelength-dependent transmission loss of PSS solution (PSS 400K) measured using a UV-vis spectrophotometer (CARY). The average transmission in the presence of 100 mg/mL of PSS 400K solution was about 17% less than that in deionized water due to partial absorption and partial scattering. However, the scattering effect was minimized by adopt-

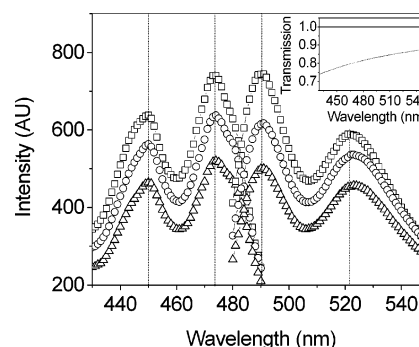


Figure 1. Fluorescence emission and excitation spectra from polystyrene latex nanoparticles impregnated with the fluorescent dye, Lumogen F Yellow 083, suspended in deionized water without added poly(styrenesulfonate) (\square), with poly(styrenesulfonate) 35K at the concentration 80 mg/mL (\circ), and with poly(styrenesulfonate) 400K at the concentration 100 mg/mL (\triangle). The inset shows the normalized transmission efficiency of deionized water (solid line) and 100 mg/mL PSS 400K solution (dashed line).

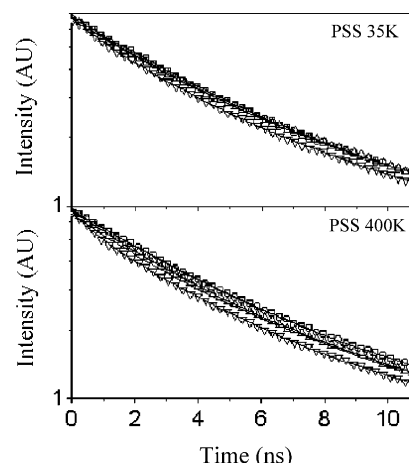


Figure 2. Fluorescence lifetime determination. The fluorescence of latex nanoparticles impregnated with Lumogen F Yellow 083 is plotted logarithmically against time on the nanosecond scale with various concentrations of poly(styrenesulfonate) (PSS) added to the suspension as indicated. The molecular weight of (PSS) is 35K (top panel) and 400K (bottom panel). Lines through the curves are second-order exponential functions. No PSS (\square); PSS 1 mg/mL (\circ); PSS 27 mg/mL (\triangle); PSS 80 mg/mL (35K), 100 mg/mL (400K) (∇).

ing two-photon excitation confocal geometry. The incident 800 nm wavelength of laser causes much less absorption by polymer sample than more conventional single photon excitation (e.g., at 400 nm), and its focal point is controlled tightly near the wall of the sample cell to minimize scattering.

Fluorescence lifetime is more sensitive to the environment. This quantity was measured with various concentrations of PSS, as shown in Figure 2. All curves were shifted to the same peak position for better comparison and were well fitted with second-order exponential decays. Fluorescence lifetime can be affected by many factors such as temperature, pH, fluorescence quenching, solvent quality, and energy transfer. However, it is known that homo energy transfer does not affect the fluorescence lifetime.¹⁸ Also, the other factors just listed, except surface-induced fluorescence quenching, would not affect the lifetime of dyes contained inside hydrophobic colloid particles because the dyes are protected by the latex shell, and all other conditions are the same except PSS concentration. The

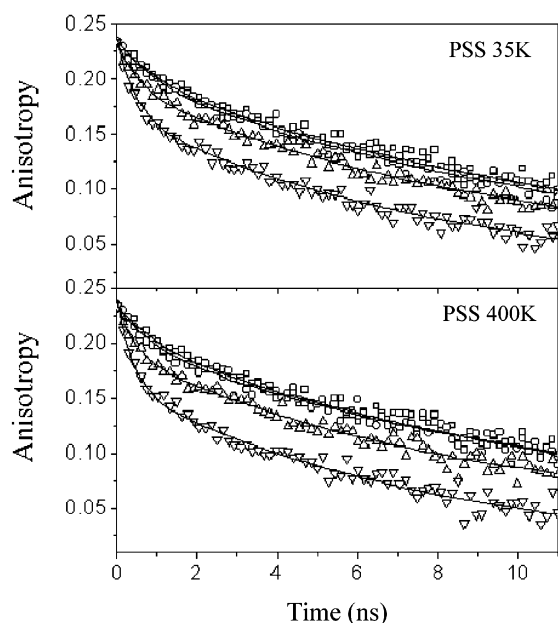


Figure 3. Fluorescence depolarization determination. The time-resolved fluorescence polarization of latex nanoparticles impregnated with Lumogen dye are plotted logarithmically against time on the nanosecond time scale with various concentrations of poly(styrenesulfonate) (PSS) added to the suspension as indicated. The molecular of PSS is 35K (top panel) and 400K (bottom panel). Lines through the curves are second-order exponential functions. No PSS (\square); PSS 1 mg/mL (\circ); PSS 27 mg/mL (Δ); PSS 80 mg/mL (35K), 100 mg/mL (400K) (∇).

only plausible mechanism to decrease the lifetime is surface-induced fluorescence quenching due to the reduction of the particle size caused by osmotic pressure¹ or electrostatic repulsion.

Figure 3 shows fluorescence depolarization traces plotted against various PSS concentrations on the nanosecond time scale. Again, all curves were shifted to the same peak position to compare the decays better. Anisotropy, r , is defined as

$$r \equiv (I_{VV} - GI_{VH}) / (I_{VV} + 2GI_{VH}) \quad (2)$$

where G is a compensating factor for the signals obtained from the detector with different sensitivity depending on polarization as described elsewhere,⁷ I is intensity, the first subscript refers to the laser polarization, and the second subscript refers to the direction of fluorescence polarization. For example, I_{VH} is the intensity of horizontally polarized fluorescence excited by a vertically polarized laser beam.

When, homo transfer occurs, it strongly depolarizes fluorescence emission because of the exchange of intermolecular interaction between an initially excited, oriented molecule, and randomly oriented neighbors. The fluorescence anisotropy decay for an ensemble of randomly oriented immobilized dyes is affected by this energy transfer as follows:¹⁷

$$r(t) = r(0) \exp \left[-g_{\text{stat}} \left(\frac{4}{3} \pi R_0^3 \rho \right) \sqrt{\frac{\pi}{2}} \frac{t}{\tau_D} \right] \equiv r(0) \exp \left[-\frac{\text{const} \sqrt{t}}{d^3} \right] \quad (3)$$

where ρ is average dye concentration, τ_D is natural fluorescence lifetime, d is the diameter of the latex

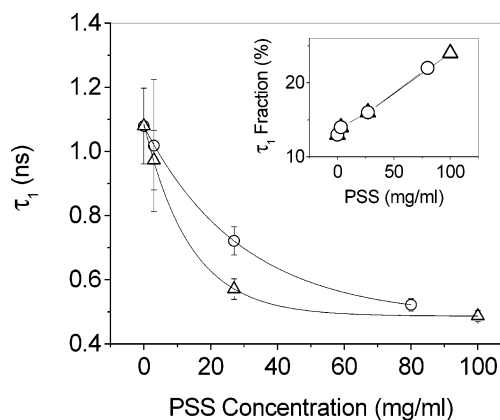


Figure 4. Time constant of the faster fluorescence depolarization process plotted against PSS concentration for PSS 35K (\circ) and PSS 400K (Δ). This was obtained from fit of the raw data to a second-order exponential function and fixing the longer time constant ($\tau_2 = 16.8$ ns). The inset shows the weighted fraction of the fast depolarization component as the PSS concentration varies. Lines through the curves in this figure are guidance for the eyes.

particle, and g_{stat} is the orientational average of the mutual orientation of two interacting molecules over the dye ensemble and is 0.8452 for immobilized, isotropically distributed dyes. The depolarization decays plotted in Figure 3 show two regimes: fast depolarization in the earliest stages, followed by a slower process. The fast depolarization became faster as PSS concentration increased while the slower depolarization was almost independent of the PSS concentration. We interpret the rapid process as homo energy transfer between immobilized dyes and the slower process as the onset of reorientation of the dyes themselves. For this reason, in the analysis below we focus only on the most rapid depolarization.

All depolarization decays were fitted by second-order exponential decay functions using PicoQuant FluorFit software (PicoQuant GmbH). For the colloid samples without PSS, the longer rotational correlation time constant was calculated to 16.8 ns. Since all the curves in Figure 3 show the same rate of depolarization decay after 2 ns, for subsequent analysis the longer time constant was fixed to 16.8 ns to consider the effect of fluorescence energy transfer on the earliest fluorescence depolarization. The origin of the slow rotational motion is attributed to the internal relaxation of dye molecules in the hydrophobic core; this is reasonable since the rotation of the colloid particle itself is vastly slower (on the order of milliseconds) and that of free dyes in water is much faster (on the order of nanoseconds).¹⁷

Figure 4 contrasts the time constants of the fast depolarization process when the suspension contained various concentrations of PSS. The decrease of time constants for the fast depolarization was more apparent in lower PSS concentration. This implies that the decrease of particle size with the addition of PSS eventually saturates, presumably due to steric repulsion. Also, the fraction of fast depolarization component (its weight in the complete depolarization process) increased with PSS concentration and was almost the same regardless of the molecular weight of PSS.

NaCl was added to PSS 400K solution (100 mg/mL concentration) as a control experiment to test whether the size changes were caused by electrostatic repulsion or not; the amount of NaCl added is shown in the figure caption. Figure 5 shows that the fast depolarization time

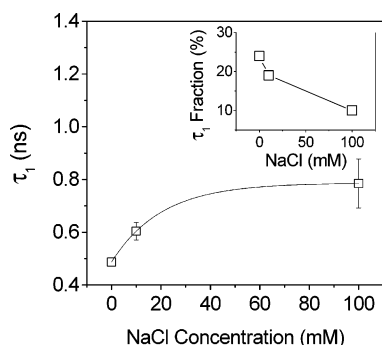


Figure 5. Time constant of the faster fluorescence depolarization process for PSS 400K (100 mg/mL) plotted against NaCl concentration in solution. This was obtained from a fit of the raw data to a second-order exponential function and fixing the time constant of the slower fluorescence depolarization process ($\tau_2 = 16.8$ ns). The inset shows the weighted fraction of the faster depolarization process, plotted against NaCl concentration in solution.

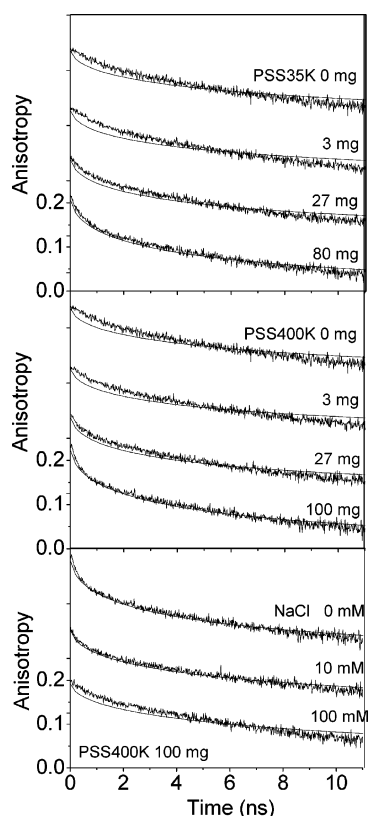


Figure 6. Fluorescence depolarization decay of Lumogen dye labeled latex nanoparticle is plotted against time with various concentrations of added PSS of which the molecular weight is 35K (top panel) and 400K (middle panel). Lower panel displays the fluorescence depolarization when NaCl is added to a PSS 400K 100 mg/mL solution. All curves were fitted by eq 3.

constant increased as NaCl concentration increased, presumably due to the screening effect of counterions. However, the fast time constant was not fully recovered at the 100 mM concentration of NaCl. The inset of Figure 5 shows that the fraction of the total depolarization contained in the fast process decreased with increasing ionic strength, presumably due to less energy transfer.

All decay curves were fitted using eq 3 to infer the change of latex particle size. Upper and middle panels of Figure 6 show that the depolarization decays at the higher concentrations of PSS were better fitted than at

the lower concentrations. The deviation of the prediction for lower PSS concentrations implies that fluorescence energy transfer is not significant in this regime of low PSS concentration. Also, the larger deviation at higher NaCl concentration shown in lower panel of Figure 6 confirms that the energy transfer is affected by the electrostatic interaction between PSS and the particles. The particle size can be calculated using eq 4

$$\frac{d}{d_0} = \left(\frac{k_0}{k}\right)^{1/3} \quad (4)$$

where d_0 is a diameter of particle without PSS and k_0 is obtained by fitting the decay curve without PSS.

Although the qualitative conclusion of shrinkage is clear, quantification is still tentative at this stage. At the lowest concentration of poly(styrenesulfonate), the fit of data to the model was imperfect, as may be seen in Figure 6, resulting in overestimation of the size change. If we consider k_0 obtained from data with 27 mg/mL of PSS where the fitting is better than that without PSS, the size of the particles at 100 mg/mL of PSS is about 2% smaller than the reference for both samples, those of molecular weight of 35 000 g/mol and also 400 000 g/mol. The recovery of the size by the addition of NaCl is also overestimated due to the deviation of the fitting at high concentration of NaCl, as may be seen in the lower panel of Figure 6. On the basis of relatively good fitting results from 0 mM NaCl in the lower panel of Figure 6, we conclude tentatively that the particle size was increased by 7% by the addition of 10 mM NaCl. On physical grounds it is likely that the volume change of these latex nanoparticles took place preferentially in interfacial regions where charged elements were more abundant, but at present we have no direct experimental evidence on this point.

In summary, time-resolved fluorescence depolarization by two-photon excitation has been used, for the first time to the best of our knowledge, to study the size change of colloid particles surrounded by highly charged polyelectrolyte. The addition of NaCl confirmed that the size change resulted from electrostatic interaction between colloids and PSS. Although the quantitative calculation is tentative in view of the simplicity of the model and the limitation of the commercially available colloid particles with dyes, we emphasize that because of the spatial resolution of two-photon fluorescence excitation, this method can be used to estimate the size changes of particles in situ in concentrated semiturbid solutions.

Acknowledgment. This work was supported by the U.S. Department of Energy, Division of Materials Science, under Award DEFG02-02ER46019, through the Frederick Seitz Materials Research Laboratory at the University of Illinois at Urbana–Champaign.

References and Notes

- (1) Saunders, B.; Vincent, B. *Colloid Polym. Sci.* **1997**, *275*, 9.
- (2) Huang, Y.; Sun, Z.; Seivick-Muraca, E. *Langmuir* **2002**, *18*, 2048.
- (3) Caruso, F.; Lichtenfeld, H.; Donath, E.; Mohwald, H. *Macromolecules* **1999**, *32*, 2317.
- (4) Heimer, S.; Tezak, D. *Colloid Interface Sci.* **2002**.
- (5) Prescott, J.; Rowell, R.; Bassett, D. *Langmuir* **1997**, *13*, 1978.
- (6) Zhao, J.; Bae, S.; Xie, F.; Granick, S. *Macromolecules* **2001**, *34*, 3123.
- (7) Lakowicz, J. *Principles of Fluorescence Spectroscopy*, 2nd ed.; Plenum Publisher: New York, 1999.

- (8) Birch, D.; Geddes, C. *Phys. Rev. E* **2000**, 62, 2977.
- (9) Karolin, J.; Geddes, C.; Wynne, K.; Birch, D. *Meas. Sci. Technol.* **2002**, 13, 21.
- (10) Otake, K.; Webber, S.; Munk, P.; Johnson, K. *Langmuir* **1997**, 13, 3047.
- (11) Goodwin, J.; Ottewill, R.; Harris, N.; Tabony, J. *J. Colloid Interface Sci.* **1980**, 78, 253.
- (12) Clegg, R.; Murchie, A.; Lilley, D. *Biophys. J.* **1994**, 66, 99.
- (13) Runnels, L.; Scarlata, S. *Biophys. J.* **1995**, 69, 1569.
- (14) Teale, F. *Photochem. Photobiol.* **1969**, 10, 363.
- (15) Lentz, B.; Moore, B.; Barrow, D. *Biophys. J.* **1979**, 25, 489.
- (16) Dorado, A.; Llorente, M.; Pierola, I. *J. Photochem. Photobiol. A* **1994**, 78, 193.
- (17) Lettinga, M.; Zandvoort, M.; Kats, C.; Philipse, A. *Langmuir* **2000**, 16, 6156.
- (18) Gautier, I.; Tramier, M.; Durieux, C.; Coppey, R.; Pansu, R.; Nicolas, J.; Kemnitz, K.; Coppey-Moisand, M. *Biophys. J.* **2001**, 80, 3000.

MA0359640